NIPPON STEEL TECHNICAL REPORT No. 136 JULY 2026

Technical Report

Characterization of Fine Precipitates by Atomic Resolution Transmission Electron Microscopy

Shunsuke TANIGUCHI* Miyuri KAMEYA

Abstract

Hydrogen trapping by alloy carbides has attracted attention as a countermeasure against delayed fracture associated with the strengthening of steel materials. In this paper, we introduce transmission electron microscopy techniques that reveal the characteristics of alloy carbides contributing to hydrogen trapping in Mo-added steels. We demonstrate that these techniques can clarify the distribution, shape, and number density of fine alloy carbides, as well as the coherency at interfaces and crystal structure of the carbides. Furthermore, it is shown that the information obtained through these techniques is beneficial for discussing hydrogen trap sites of alloy carbides.

1. Introduction

Steel materials are widely used as fundamental structural materials supporting modern society. To achieve weight reduction and enhanced safety, further strengthening of the steel materials is required. However, in practical applications, not only strength but also other mechanical properties, such as elongation and toughness, must be satisfied in a balanced manner. The mechanical properties are strongly influenced by microstructural features, such as crystal grains, inclusions, dislocations, precipitates, and solute elements. Therefore, advanced characterization techniques are essential for investigating the relationship between microstructures and mechanical properties.

Transmission electron microscopy (TEM) uses a high-energy electron beam to irradiate thin specimens, typically less than 100 nm thick. TEM enables imaging, crystallographic analysis, and chemical analysis. Scanning transmission electron microscopy (STEM) is a TEM-based technique in which a fine focused electron beam scans the specimen, allowing localized analysis at selected positions. By adjusting the detection angles of annular detectors, the diffraction contrast can be controlled. Recent advances in aberration corrected electron optics significantly improved spatial resolution, making atomic-scale analysis possible. TEM and STEM are therefore well-suited for investigating grain boundaries, interfaces, and fine precipitates in the steel materials.

As the tensile strength of steel materials exceeds 1 200 MPa, hydrogen-induced delayed fracture becomes a serious concern. One proposed method to suppress the delayed fracture is to trap absorbed hydrogen using nanometer-sized alloy carbides precipitated during tempering martensitic structures at relatively high temperatures.[1, 2)]

Hydrogen trapping by B1-type alloy carbides, represented by TiC (hereafter referred to as MC carbides), has been extensively studied.[3–10)] Proposed hydrogen trapping sites include misfit dislocations at coherent and semi-coherent interfaces, C vacancies at interfaces, and C vacancies within the alloy carbides. High-strength quenched-and-tempered bolts commonly contain Mo and V additions. While V forms the same MC carbides as TiC, Mo forms hexagonal close-packed (HCP) Mo_2C carbides (hereafter referred to as M_2C carbides).[11)] M_2C carbides precipitate as needle-shaped structures with a Pitch-Schrader orientation relationship with the ferrite matrix.[12)] Previous studies have reported hydrogen trapping at coherent interfaces of the needle-shaped M_2C carbides in Mo-added steels.[13, 14)] More recently, MC carbides have also been observed in Mo-added steels and suggested to act as hydrogen trapping site.[15)] However, detailed atomic-scale analysis of the MC and M_2C carbides in Mo-added steels remains limited, and the dominant hydrogen trap sites are still unclear.

We investigated how fine Mo carbides contribute to hydrogen trapping in Mo-added steel.[16)] In this paper, we introduce advanced TEM techniques that have clarified the characteristics of alloy carbides responsible for hydrogen trapping.

2. Hydrogen Trapping Behavior in Mo-added Steel

First, we introduce the hydrogen trapping behavior of Mo-added steel, comparing it with V-added steel in which MC carbides are

* Senior Researcher, Materials Characterization Research Lab., Advanced Technology Research Laboratories
1-8 Fuso-cho, Amagasaki City, Hyogo Pref. 660-0891

known to precipitate. An Fe-0.1C-2Mn-1.6Mo (mass%) alloy (hereafter referred to as Mo steel) was used as the steel material for precipitating Mo carbides.[17] For comparison, an Fe-0.1C-2Mn-0.55V (mass%) alloy (hereafter referred to as V steel) was prepared. Round bars were heated to 1 373 K for 3.6 ks to fully dissolve Mo and V, followed by oil quenching. Tempering was conducted at 873 K for durations ranging from 1.8 ks to 36 ks.

Cylindrical specimens with a diameter of 7 mm were taken from both the as-quenched round bars and the tempered round bars for hydrogen analysis. Hydrogen content was measured using thermal desorption analysis (TDA) with a gas chromatograph as the detection system. Hydrogen charging was carried out by cathodic electrolysis in an aqueous solution of 3% NaCl + 3 g/L NH_4SCN at a current density of 0.2 mA cm^{-2} for 259.2 ks. After aging at room temperature for 172.8 ks, the remaining hydrogen in the specimens was measured by TDA during heating from room temperature to 773 K at a rate of 0.028 K s^{-1} (100 K h^{-1}). The measured hydrogen content was defined as trapped hydrogen.

Figure 1 shows the variation of Vickers hardness with tempering time. In Mo steel, the as-quenched specimen (AsQ) has hardness of 321. Hardness increasing by tempering and reaches a peak at 7.2 ks, followed by a monotonic decrease. In contrast, V steel exhibits a continuous increase in hardness up to 14.4 ks remaining harder than the as-quenched state at longer tempering time. The hardness-tempering time relationship differs between Mo steel and V steel.

Figure 2 presents the relationship between trapped hydrogen content and tempering time. In both steels, the trapped hydrogen content is less than 0.2 mass ppm in the as-quenched state. In Mo steel, the trapped hydrogen content reaches a maximum at 1.8 ks and decreases monotonically with increasing tempering time. In contrast, V steel shows a significant increase in trapped hydrogen between 3.6 ks and 7.2 ks, after which the hydrogen content remains approximately constant at ~6 mass ppm. Similar to the hardness dependence on tempering time, trapped hydrogen behavior also differs significantly between Mo steel and V steel.

3. Atomic-scale Analysis of Mo Carbides by TEM

To clarify the origin of the observed differences in hydrogen trapping behavior, alloy carbides within martensitic laths were analyzed by TEM. Mo steels tempered for 3.6 ks and 14.4 ks were examined to evaluate the effect of tempering time. V steel tempered for 14.4 ks was also analyzed for comparison.

In **Fig. 3**, low-angle annular dark-field (LAADF) STEM images were acquired using detector angles of 19–80 mrad, together with elemental maps obtained by energy-dispersive X-ray spectroscopy (EDS). In LAADF-STEM images, diffraction contrast contributes strongly, allowing dislocations and precipitates to appear as bright features.[18, 19] While EDS mapping requires relatively long acquisition times of approximately 600 s to 3.6 ks to obtain a sufficient signal level, a single LAADF-STEM image can be acquired within about 60 s. LAADF-STEM imaging is suitable for visualizing the spatial distribution of alloy carbides over wide areas.

Figures 3 (a, b) correspond to Mo steel tempered for 3.6 ks, Fig. 3 (c, d) to Mo steel tempered for 14.4 ks, and Fig. 3 (e, f) to V steel

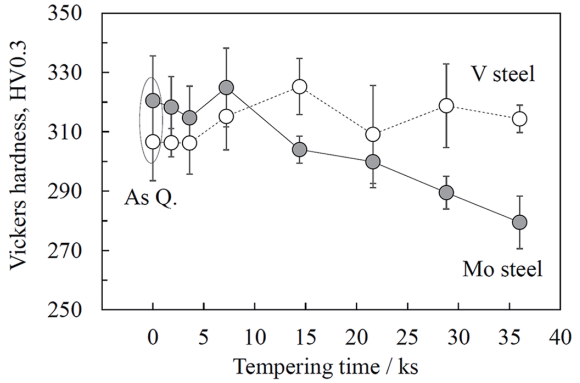

Fig. 1 Effect of tempering time to Vickers hardness of Mo steel and V steel tempered at 873 K[16]

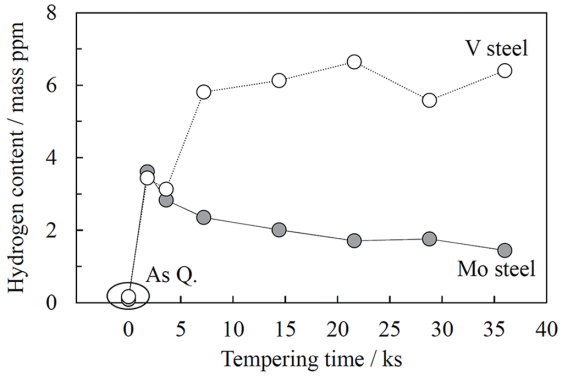

Fig. 2 Relationship between hydrogen content and tempering time at 873 K[16]

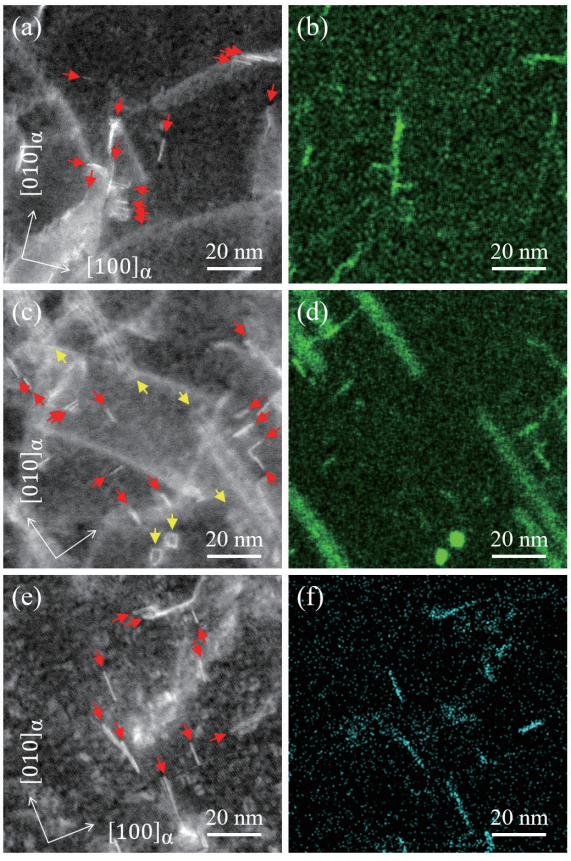

Fig. 3 LAADF-STEM images of alloy carbides and elemental maps of Mo and V[16]

tempered for 14.4 ks. The bright, granular contrast in the LAADF-STEM images of Fig. 3(a, c, e) corresponds to the enrichment observed in Fig. 3(b, d) for Mo and in Fig. 3(f) for V. It represents alloy carbides. In the LAADF-STEM images of Fig. 3(a, c, e), plate-like alloy carbides are indicated by red arrows. In addition, needle-like Mo carbides, indicated by yellow arrows, precipitate in Mo steel tempered for 14.4 ks, as shown in Fig. 3(c). These observations demonstrate that two types of alloy carbides precipitate in the Mo steel.

To clarify the crystal structure of the alloy carbides and the coherency of their interfaces, high-angle annular dark-field (HAADF) STEM images were acquired with detector angles of 80–200 mrad. While high-resolution TEM images yield lattice patterns via phase contrast, image simulation is essential to establish correspondence with atomic columns. In contrast, atomic columns always appear as bright features in HAADF-STEM images, enabling intuitive interpretation of atomic structures.[20] Furthermore, the crystal structure can be discussed based on the Fourier transform pattern of the atomic resolution image.

Figure 4 shows atomic-resolution HAADF-STEM images of alloy carbides and their fast Fourier transform (FFT) patterns. Figure 4(a, b) correspond to Mo steel tempered at 3.6 ks, Fig. 4(c–f), to Mo steel tempered at 14.4 ks, and Fig. 4(g, h), to V steel tempered at 14.4 ks. Figures 4(a), (c), and (g) are examples of HAADF-STEM images of the plate-like alloy carbides indicated by red arrows in Fig. 3. Across the broad plate interface, the arrangement of Fe atomic columns corresponds one-to-one with that of Mo or V atomic columns, as indicated by the yellow dashed lines. The broad interface of the plate-like alloy carbide is coherent. Furthermore, the FFT patterns in Fig. 4(b, d, h) confirm that the alloy carbide is an MC carbide with Baker-Nutting orientation relationship. Figure 4(e) shows an example of an HAADF-STEM image of the needle-like Mo carbide indicated by the yellow arrow in Fig. 3(c). A mismatch is observed between the Fe atomic columns in the matrix and the Mo atomic columns in the carbides, indicating the presence of misfit dislocations, as denoted by the symbol ⊥. This demonstrates that the side interfaces of the needle are not coherent interfaces. The FFT pattern in Fig. 4(f) identifies these needle-like Mo carbides as M_2C carbides with a Pitch-Schrader orientation relationship.

Figure 5 summarizes the quantitative analysis of the morphology and number density of alloy carbides based on the STEM observations. For the number density evaluation, the average specimen

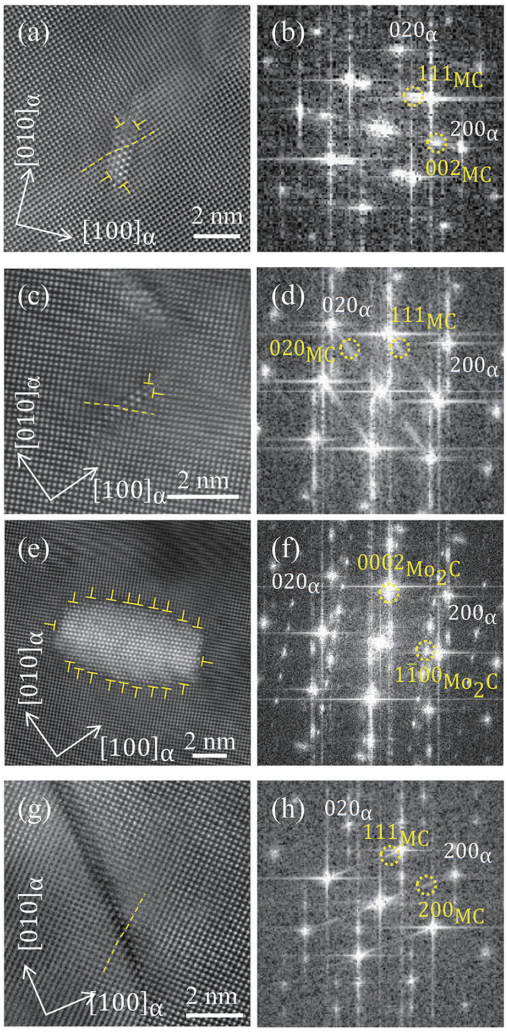

Fig. 4 Atomic resolution HAADF-STEM images of alloy carbides and fast Fourier transformed patterns[16]

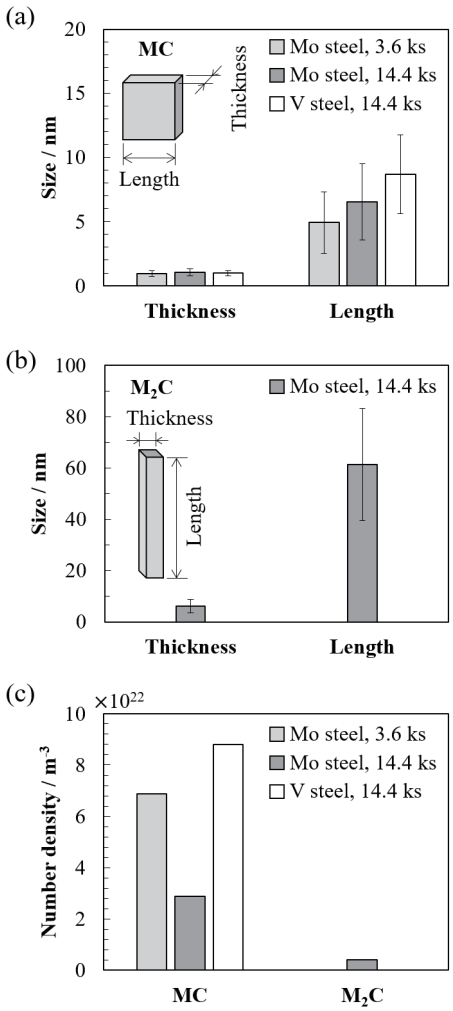

Fig. 5 Size and particle density of alloy carbides in Mo steel and V steel tempered at 873 K[16]

thickness within the observation field was measured using electron energy loss spectroscopy (EELS).[21] The definitions of length and thickness representing alloy carbides are illustrated schematically in Fig. 5. The morphology of the alloy carbides was assumed to be a rectangular parallelepiped with a square cross-section. As shown in Fig. 5(a), the average thickness of MC carbide in Mo steel remains nearly constant between tempering times of 3.6 ks and 14.4 ks, whereas the average length increases with tempering time. When comparing MC carbides in Mo steel and V steel at the same tempering time of 14.4 ks, the average thickness is nearly identical, but the average length is larger in V steel. The coherent MC carbides are considered to have stopped growing at a certain thickness and then grown in the length direction. Figure 5(b) shows only the data of Mo steel tempered for 14.4 ks, in which MC and M_2C carbide were observed. The M_2C carbides are coarser than the MC carbides. Figure 5(c) shows the number densities of MC carbides and M_2C carbides. In the Mo steel, the number density of MC carbides decreases to less than half between tempering times of 3.6 ks and 14.4 ks. Although M_2C carbides precipitate at 14.4 ks, their number density is approximately one order of magnitude lower than that of MC carbides. The number density of MC carbides in V steel tempered for 14.4 ks is higher than that in Mo steel at the same tempering time. In Mo steel, MC carbides precipitate at the early stage in tempering, but as the tempering time increases, M_2C carbides precipitate and the MC carbides decompose.

Figure 6 shows the relationship between the interfacial area of alloy carbides per unit volume and the amount of trapped hydrogen. The interfacial area was calculated based on the carbide morphology assumptions illustrated in Fig. 5. In previous studies, the broad interfaces of plate-like MC carbides[5, 7–10, 15] and the side interface of needle-like M_2C carbides[13, 14] have been proposed as hydrogen trap sites. Therefore, the interface area was calculated for these interfaces. In the Mo steel temperedfor 14.4 ks, both MC carbides and M_2C carbides were observed, so the interface areas of each carbide and their sum were plotted separately. Plots of the Mo steel tempered for 3.6 ks and the V steel tempered for 14.4 ks show MC carbide interface areas. While the Mo steel tempered for 14.4 ks has a large total interface area of MC carbide and M_2C carbide (8.8×10^6 m^2 m^{-3}), its trapped hydrogen content is relatively low at 2.0 mass ppm. When focusing solely on the MC carbide, a clear positive correlation between the interfacial area and trapped hydrogen content is observed for both Mo steel and V steel. These results suggest that the coherent, broad interface of the MC carbides in Mo steel is the primary hydrogen trap site, while both MC carbides and M_2C carbides precipitate.

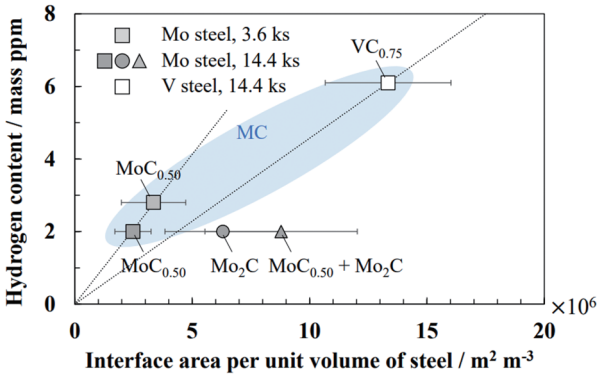

Fig. 6 Relationship between hydrogen content and interface area of alloy carbide per unit volume of Mo steel and V steel tempered at 873 K[16]

4. Conclusion

This paper introduced atomic-level structural analysis techniques using transmission electron microscopy (TEM) applied to analyze Mo carbides responsible for hydrogen trapping in Mo-added steels. The TEM techniques enable comprehensive characterization of fine alloy carbides, including their distribution, morphology, number density, interfacial coherency, and crystal structure. It demonstrated that this technique provides valuable information for discussing hydrogen trapping by alloy carbides.

References

1) Kushida, T. et al.: Tetsu-to-Hagané. 82, 297 (1996)
2) Yamasaki, S. et al.: Tetsu-to-Hagané. 83, 454 (1997)
3) Stevens, M.F. et al.: Metall. Trans. A. 16, 1879 (1985)
4) Stevens, M.F. et al.: Metall. Trans. A. 20, 909 (1989)
5) Tsuchida, T. et al.: Tetsu-to-Hagané. 88, 771 (2002)
6) Kosaka, M. et al.: CAMP-ISIJ. 17, 1370 (2004)
7) Kosaka, M. et al.: CAMP-ISIJ. 17, 1371 (2004)
8) Wei, F.G. et al.: Metall. Mater. Trans. A. 37, 331 (2006)
9) Wei, F.G. et al.: Proc. 2008 Int. Hydrogen Conf. – Effects of Hydrogen on Materials, Ohio, ASM International, 2009, p.448
10) Takahashi, J. et al.: Acta Mater. 153, 193 (2018)
11) Seal, A.K. et al.: J. Iron Steel Inst. 188, 343 (1958)
12) Dyson, D.J. et al.: Acta Metall. 14, 867 (1966)
13) Totsuka, N. et al.: Tetsu-to-Hagané. 69, A113 (1983)
14) Hinotani, S. et al.: Mater. Sci. Eng. 76, 57 (1985)
15) Kinami, T.: Tetsu-to-Hagané. 108, 656 (2022)
16) Taniguchi, S. et al.: Tetsu-to-Hagané. 109, 438 (2023)
17) Kameya, M. et al.: CAMP-ISIJ. 33, 620 (2020)
18) Chomsaeng, N. et al.: J. Alloys Compd. 496, 478 (2010)
19) Phillips, P.J. et al.: Ultramicroscopy. 116, 47 (2012)
20) Pennycook, S.J. et al.: Ultramicroscopy. 37, 14 (1991)
21) Malis, T. et al.: J. Electron Microsc. Tech. 8, 193 (1988)

Shunsuke TANIGUCHI
Senior Researcher
Materials Characterization Research Lab.
Advanced Technology Research Laboratories
1-8 Fuso-cho, Amagasaki City, Hyogo Pref. 660-0891

Miyuri KAMEYA
Researcher
Integrated Steel-Solution Research Lab.-II
Steel Research Laboratories